PERGAMON

Available online at www.sciencedirect.com

SCIENCE DIRECT®

Polyhedron 22 (2003) 67–73

POLYHEDRON

www.elsevier.com/locate/poly

Reactions of M{N(SiMe$_3$)$_2$}$_2$ (M = Mn, Fe or Co) with pyridine and 4,4′-bipyridyl: structural and magnetic studies

Arunashree Panda [a], Matthias Stender [a], Marilyn M. Olmstead [a], Peter Klavins [b], Philip P. Power [a,*]

[a] Department of Chemistry, University of California, Davis, One Shields Avenue, Davis, CA 95616, USA
[b] Department of Physics, University of California, Davis, One Shields Avenue, Davis, CA 95616, USA

Received 8 July 2002; accepted 22 September 2002

Abstract

The reactions of the aromatic nitrogen donor ligands pyridine (py) and 4,4′-bipyridyl (4,4′-bipy) with the transition metal silylamides M{N(SiMe$_3$)$_2$}$_2$ (M = Mn, Fe or Co) were investigated. Treatment of the metal amides with pyridine afforded the bispyridine complexes M{N(SiMe$_3$)$_2$}(py)$_2$ (M = Mn, **1a**; Fe, **2a**; Co, **3a**). Distillation or sublimation of **2a** or **3a** afforded the monopyridine complexes M{N(SiMe$_3$)$_2$}$_2$(py) (M = Fe, **2b**; Co, **3b**). The addition of pyrazine (prz) to Mn{N(SiMe$_3$)$_2$}$_2$ also yielded the bispyrazine adduct Mn{N(SiMe$_3$)$_2$}$_2$(prz)$_2$, **1b**. However, the reaction of 4,4′-bipyridyl with Fe{N(SiMe$_3$)$_2$}$_2$ or Co{N(SiMe$_3$)$_2$}$_2$ afforded the polymeric chain-like complexes {M{N(SiMe$_3$)$_2$}$_2$(4,4′-bipy)}$_\infty$ (M = Fe, **4**; Co, **5**). With the exception of **2b**, all complexes were characterized by X-ray crystallography. The complexes **1a**, **1b**, **2a** and **3a** displayed monomeric structures and metal geometries that are based on a tetrahedron with interligand angles that deviate markedly from idealized values. Complex **3b** was found to have a distorted trigonal planar geometry. In contrast, complexes **4** and **5** displayed polymeric zig-zag chain structures which have four coordinate metal centers connected by 4,4′-bipyridyl ligands. Magnetic studies indicated that complexes **1**–**3b** have high-spin electron configurations and that the paramagnetic centers in **4** and **5** did not interact with each other through the 4,4′-bipyridyl ligands.

Keywords: Pyridine; X-ray crystallography; Metal amide; Silyamide

1. Introduction

Transition metal silylamides of formula M{N(SiMe$_3$)$_2$}$_2$ (M = Mn [1], Fe [2] or Co [3]) have been shown to be useful precursors for a wide variety of derivatives of these metals [4]. Their utility is partly derived from the fact that they are freely soluble in hydrocarbon solvents such as hexane or benzene. In addition, they possess semi-polar, reactive metal–nitrogen bonds that can be readily cleaved by protic reagents with the elimination of volatile HN(SiMe$_3$)$_2$. As monomeric, two coordinate species, the formal electron count in their valence shells is low—nine, ten and eleven electrons for the manganese, iron and cobalt complexes, respectively. This results in considerable Lewis acid character at the metals which is manifested in the formation of complexes with Lewis bases and self association to amide bridged dimers in the crystalline phase [5–7]. Monomeric complexes of these metals with various donor ligands are known, but relatively few have been structurally characterized and described in full detail. The latter include Co{N(SiMe$_3$)$_2$}$_2$(PPh$_3$) [8], Fe{N(SiMe$_3$)$_2$}$_2$(THF) [7], Mn{N(SiMe$_3$)$_2$}$_2$(THF)$_2$ [9], Mn{N(SiMe$_3$)$_2$}$_2$(1,10-phenanthroline) [10] and [Mn{N(SiMe$_3$)$_2$}$_2$(4,4′-bipy)·THF]$_\infty$ (4,4′-bipy = 4,4′-bipyridyl) [10]. The tendency to form complexes with either one or two donor ligands is a characteristic feature of these compounds, although pairs of three and four coordinate complexes that differ only by one donor ligand of the same type remain rare. Thus, the synthesis and structure of 2:1 complex Mn{N(SiMe$_3$)$_2$}$_2$(THF)$_2$ [9] has been described in detail whereas 1:1 complex Mn{N(SiMe$_3$)$_2$}(THF) has only been

---

* Corresponding author
E-mail address: pppower@ucdavis.edu (P.P. Power).

0277-5387/02/$ - see front matter © 2002 Elsevier Science Ltd. All rights reserved.
PII: S0277-5387(02)01264-0

described in a review where the magnetic moment ($\mu_{eff} = 5.91\mu_B$) and some of the structural parameters (Mn–O = 2.16(2) Å, Mn–N = 1.99(2) Å, NMnN angles = 145° and 150°, NMnO angles were 101°–113°) [11]. In addition, an interesting aspect of the chemistry of $Mn\{N(SiMe_3)_2\}_2$ is that it has been shown to form a complex $[Mn\{N(SiMe_3)_2\}_2(4,4'\text{-bipy})\cdot THF]_\infty$, **6**, whose structure consists of zig-zag infinite chains in which the 4,4′-bipy ligands link the paramagnetic manganese centers [10]. Hydrocarbon soluble compounds of this type are of potential importance for the synthesis of ordered arrays of paramagnetic centers separated by well-defined distances. In order to explore these aspects of the chemistry further, several complexes of the amides $M\{N(SiMe_3)_2\}_2$ (M = Mn, Fe or Co) with the nitrogen donor ligands pyridine (py), 4,4′-bipyridyl (4,4′-bipy) and pyrazine (prz) have been synthesized and characterized.

2. Experimental

2.1. Synthesis

2.1.1. General procedures

All work was performed by using modified Schlenk techniques under an N_2 atmosphere or in a Vacuum Atmospheres dry box. Solvents were freshly distilled from Na–K alloy and degassed three times immediately before use. The compounds $M\{N(SiMe_3)_2\}_2$ (M = Mn, Co, Fe) were synthesized by modified literature procedures [1–3] from 'activated', anhydrous $MnCl_2$ and $FeCl_2$, which were obtained from finely powdered $MnCl_2\cdot 4H_2O$ and $FeCl_2\cdot 4H_2O$ by following a slightly modified version of the procedure reported by Horvath [12], or commercially available anhydrous $CoCl_2$ (Aldrich). 1,1,1,3,3,3,-hexamethyldisilazane, 98% (Aldrich) and pyrazine (prz) were used as received. Pyridine (py) was distilled under reduced pressure over molecular sieves prior to use. Infrared spectra were obtained as Nujol mulls with a Perkin–Elmer-1430 spectrometer. Electronic absorption spectra were obtained on a Hitachi U-2000 UV–Vis spectrophotometer. Melting points (m.p.) are uncorrected and were determined for samples in capillaries sealed with grease. For magnetic measurements the samples were sealed under vacuum in 3.2 × 2 mm quartz tubing. The sample holder was designed to minimize the background signal. The sample magnetization was measured using a Quantum Design [13] MPMSXL7 superconducting quantum interference device (SQUID) magnetometer. For each measurement, the sample was zero-field cooled to 5 K and the magnetization was measured as a function of field to 2 T. The field was then reduced to 1 T and the magnetization of the sample was measured in 5 K increments to 300 K.

2.2. $Mn\{N(SiMe_3)_2\}_2(py)_2$ (**1a**)

At 25 °C, $Mn\{N(SiMe_3)_2\}_2$ (0.75 g, 2 mmol) was dissolved in hexane (20 ml), and a solution of pyridine (1.6 ml, tenfold excess) in hexane (10 ml) was added via a canula with rapid stirring. The color of the solution immediately changed from pale pink to yellow. The solution was concentrated to approximately 10 ml under reduced pressure and stored in a approximately −20 °C freezer for 20 h. The product was obtained as very pale yellow, almost colorless crystals. Yield: 0.56 g, 1.05 mmol, 52%. M.p. 106–108 °C; IR (Nujol, cm^{-1}): 2940, 2920, 2840, 1600, 1460, 1380, 1262, 1152, 1070, 1015(b), 800(b), 700, 660, and 360. UV–Vis (hexane, λ_{max} nm (ε, M^{-1} cm^{-1}): 227 (14 000) 335 (16 500). $\mu = 5.90(2)\mu_B$.

2.3. $Mn\{N(SiMe_3)_2(prz)_2$ (**1b**)

This compound was prepared on a 2 mmol scale as pale yellow crystals by a procedure similar to that employed for **1a**. Yield: 0.49 g, 0.91 mmol, 46%. M.p. 90–91 °C; IR (Nujol, cm^{-1}): 2930, 2840, 1602, 1450, 1376, 1260, 1220, 1160, 1130, 980, 830, 755, 695, 675, 620, and 355. $\mu = 5.85(2)\mu_B$.

2.4. $Fe\{N(SiMe_3)_2\}_2(py)_2$ (**2a**)

At 25 °C, $Fe\{N(SiMe_3)_2\}_2$ (0.75 g, 2 mmol) was dissolved in hexane (20 ml) to form a green solution. Pyridine (1.6 ml, tenfold excess) in hexane (20 ml) was added via a canula with rapid stirring. The color of the solution immediately changed from green to red. After stirring for 1 h, the volume of the solution was reduced to approximately 10 ml. Storage in a −20 °C freezer for 40 h afforded the product as red crystals. Yield: 1.0 g, 1.87 mmol. M.p. 72–74 °C. IR (Nujol, cm^{-1}): 2940(b), 2840, 1600, 1450(m), 1375, 1255, 1245, 1210, 1070, 1040, 980(b), 830(b), 750, 690, 670, 630, 610, and 355. UV–Vis: 275 (15 000), 399 (250). $\mu = 5.48(2)\mu_B$.

2.5. $Fe\{N(SiMe_3)_2\}_2(py)$ (**2b**)

This compound was obtained by sublimation of red crystals of **2a** at approximately 100 °C and 0.01 mm Hg. The product **2b** was isolated as green crystals in approximately 80% yield. M.p. 84–86 °C. IR (Nujol, cm^{-1}): 2930, 1605, 1465, 1380, 1260, 1290, 1150, 1072, 1040, 980, 830, 750, 693, 675, 632, 615 and 362. $\mu = 5.31(2)\mu_B$.

2.6. $Co\{N(SiMe_3)_2\}_2(py)_2$ (**3a**)

This was prepared in a manner similar to the manganese and iron species, **1a** and **2a**. In this case, the color changed from yellow–green to blue–green upon addition of excess pyridine. Yield: 0.68 g, 62%.

M.p. 58–60 °C. IR (Nujol, $\mathrm{cm^{-1}}$): 2940, 2910, 2840, 1600, 1480, 1450, 1260, 1210, 1180, 1150, 1090(b), 1065, 1015(b), 1030, 800(m), 750, 690, 610(m) and 360. UV–Vis: (14 200), 648 (350), 694 (300). $\mu = 4.65(3)\mu_B$.

2.7. *Co{N(SiMe$_3$)$_2$}$_2$(py) (**3b**)*

The compound was prepared by sublimation of crystals of **3a** at approximately 100 °C and 0.01 mm Hg. The product was isolated as blue–green crystals that proved suitable for X-ray crystallographic studies. Yield: 69%. M.p. 110–112 °C. IR (Nujol, $\mathrm{cm^{-1}}$): 1600, 1450, 1375, 1255, 990, 810, 750, 695, 665, 610, and 360. UV–Vis: 318, 383, 647 and 696 nm. $\mu = 4.69\mu_B$.

2.8. *[Fe{N(SiMe$_3$)$_2$}$_2$(4,4′-bipy)]$_\infty$ (**4**)*

$\mathrm{Fe\{N(SiMe_3)_2\}}$ (0.75 g, 2 mmol) was dissolved in approximately 20 ml of hexane and this was added to 4,4′-bipyridyl (0.31 g, 2 mmol) in hexane (10 ml) via canula at room temperature (r.t.). Immediately a blue precipitate was formed. It was allowed to stir at 25 °C overnight whereupon the solvent was removed under pressure. The residue was redissolved in approximately 30 ml of toluene with heating. Upon cooling it afforded blue needles suitable for X-ray crystallographic studies. Yield: 1 g, 93%. M.p. 184–186 °C. IR (Nujol, $\mathrm{cm^{-1}}$): 2940, 2910, 2840, 1600, 1530, 1480, 1460(b), 1405, 1375, 1260, 1175, 1090(b), 1060, 1020(b), 970, 960, 800, 745, 600 and 360. $\mu = 4.44\mu_B$.

2.9. *[Co{N(SiMe$_3$)$_2$}$_2$(4,4′-bipy)]$_\infty$ (**5**)*

The synthesis was accomplished in a manner similar to the preparation of **4** with use of $\mathrm{Co\{N(SiMe_3)_2\}_2}$ (0.76 g, 2 mmol) and 4,4′-bipyridyl (0.31 g, 2 mmol). Green crystals suitable for X-ray crystallographic studies were obtained from toluene. Yield: 0.95 g, 89%. M.p. 173–178 °C. IR (Nujol, $\mathrm{cm^{-1}}$): 1605, 1530, 1486, 1465, 1410, 1380, 1310, 1260, 1240, 1215, 1065, 980–810, 665, 630, 610, 460 and 360. $\mu = 3.76\mu_B$.

2.10. *X-ray data collection and refinement*

X-ray quality crystals of **1**–**5** were removed from the Schlenk tube under a stream of N_2 and immediately covered with a layer of hydrocarbon oil. Suitable crystals were selected, attached to glass fibers and placed in the cold temperature N_2-stream as previously described [14]. The data were collected near 90 or 130 K using a Bruker Smart 1000 (**1**–**4**) or Siemens R3m/V diffractometer (**5**) with Mo Kα ($\lambda = 0.71073$ Å) for **1**–**4** or Cu Kα ($\lambda = 1.54178$ Å) for **5**. The SHELXTL version 5.1 program package [15] was used for the structure solutions and refinements (**1**–**4**). Absorption corrections were applied using the SADABS or XABS2 program [16a,16b]. Calculations for **5** were performed on a MicroVax 3200 using the SHELXTL PLUS program system. The structures were solved by direct methods and refined by full-matrix least-squares procedures. All non-hydrogen atoms were refined anisotropically. Hydrogen atoms were included in the refinement at calculated positions using a riding model. Some details of the data collection and refinement are given in Table 1. Selected bond distances and angles for **1**–**5** are provided in Table 2.

3. Discussion

3.1. *Synthesis*

The compounds **1**–**5** were synthesized in a facile manner by direct addition of the nitrogen donor Lewis bases to the amides. The addition of excess pyridine to $\mathrm{M\{N(SiMe_3)_2\}_2}$ (M = Mn, Fe or Co) afforded the bispyridine complexes **1a**, **2a**, and **3a** as air sensitive crystals in 52–94% yields. Sublimation of the complexes **2a** and **3a** at 100 °C and approximately 0.01 mm Hg afforded crystals of the monopyridine complexes **2b** and **3b**. Attempted recrystallization of **2b** or **3b** from hexane can result in the isolation of crystals of **2a** and **3a**. Presumably, an equilibrium described by Eq. (1) exists in this solvent at room temperature which is driven by the somewhat lower solubility of **2a** and **3a**:

$$\underset{\mathbf{2b}\ \text{or}\ \mathbf{3b}}{2\mathrm{M\{N(SiMe_3)_2\}_2(py)}} \rightleftarrows \underset{\mathbf{2a}\ \text{or}\ \mathbf{3a}}{\mathrm{M\{N(SiMe_3)_2\}_2(py)_2}} + \mathrm{M\{N(SiMe_3)_2\}_2} \qquad (1)$$

Similar behavior has been observed for THF complexes of $\mathrm{Mn\{N(SiMe_3)_2\}_2}$ where $\mathrm{Mn\{N(SiMe_3)_2\}_2(THF)_2}$ can be obtained from THF solution whereas the mono adduct $\mathrm{Mn\{N(SiMe_3)_2\}_2THF}$ is obtained on sublimation [9]. Parallel behavior has been recently reported for substituted pyridine adducts of $\mathrm{Mg\{N(SiMe_3)_2\}_2}$ where $\mathrm{Mg\{N(SiMe_3)_2\}_2(THF)_2}$ was shown to form the bis complexes $\mathrm{Mg\{N(SiMe_3)_2\}_2(L)_2}$ (L = 2,3,5-collidine, 2-picoline, 4-picoline, 3,5-butidine) upon treatment with 2 equiv. of the substituted pyridines L [17]. Sublimation of the bis 2,3,5-collidine and 2-picoline complexes afforded the corresponding three coordinate 1:1 complexes. Complexes of $\mathrm{Co\{N(SiMe_3)_2\}_2}$ (L′) with L′ = pyridine, 4-picoline and 2,4-dimethylpyridine have been reported previously but they were not structurally characterized [18]. They were prepared by the reaction of excess of base with $\mathrm{Co\{N(SiMe_3)_2\}_2}$ in benzene. It was reported that $\mathrm{Co\{N(SiMe_3)_2\}_2(L')}$ could be obtained by distillation or recrystallization from hexane. The work reported in this paper confirms the former method. However, it was found that attempted recrystallization of **2b** and **3b** from hexane led to the isolation of **2a** and **3a**. It is

Table 1
Data collection parameters for **1**–**5**

	1a	**1b**	**2a**	**3a**	**3b**	**4**	**5**
Formula	$C_{22}H_{46}MnN_4Si_4$	$C_{20}H_{44}MnN_6Si_4$	$C_{22}H_{46}FeN_4Si_4$	$C_{22}H_{46}CoN_4Si_2$	$C_{17}H_{41}CoN_3Si_4$	$C_{22}H_{44}FeN_4Si_4$	$C_{22}H_{44}MnN_4Si_4$
Formula weight	533.93	535.91	534.84	537.92	453.82	532.82	531.91
Crystal system	monoclinic	monoclinic	monoclinic	monoclinic	orthorhombic	monoclinic	monoclinic
Space group	$P2_1/c$	$P\bar{1}$	$P2_1/c$	$P2_1/c$	$Pbcn$	$C2/c$	$C2/c$
a (Å)	13.077(7)	8.591(4)	13.0211(7)	12.9660(6)	13.265(2)	20.488(9)	20.419(4)
b (Å)	11.7179(6)	11.295(5)	11.6864(6)	11.6776(6)	11.213(2)	9.302(2)	9.338(1)
c (Å)	20.3539(11)	16.905(6)	20.322(1)	20.230(1)	17.803(2)	17.655(7)	17.8305
α (°)		75.23(3)					
β (°)	90.464(1)	76.43(3)	90.494(1)	90.541(1)		118.69(3)	118.09(2)
γ (°)		75.58(3)					
V (Å^3)	3109.5(3)	1510.3(11)	3092.3(3)	3062.9(3)	2648.1(6)	2952(2)	2999.3(11)
Z	4	2	4	4	4	4	4
μ (Mo Kα) (mm^{-1})	0.594	0.614	0.658	0.733	0.835	0.690	5.225
T (K)	90(2)	130(2)	90(2)	90(2)	91(2)	130(2)	130(2)
R_1	0.026	0.036	0.027	0.029	0.052	0.041	0.0454
wR_2	0.0706	0.0743	0.073	0.074	0.1067	0.0838	0.0893

$R_1 = \Sigma||F_o| - |F_c||/|F_o|$; $wR_2 = [\Sigma\omega(F_o^2 - F_c^2)^2/\Sigma[\omega(F_o^2)]]^{1/2}$.

notable that the pairs of compounds **3a**, **3b** hardly differ in color and it is difficult to distinguish between the mono and bispyridine complexes visually. The isolation of three coordinate species **2b** and **3b** show that complexation with one pyridine does not saturate the coordination sphere. The unsaturation is reflected in the extreme air sensitivity of these complexes. The addition of 1 equiv. of 4,4′-bipyridyl to Fe{N(SiMe$_3$)$_2$}$_2$ or Co{N(SiMe$_3$)$_2$}$_2$ afforded the complexes **4** and **5** in excellent yields similar to the previously published Mn{N(SiMe$_3$)$_2$}$_2$(4,4′-bipy) [10]. Attempts at synthesizing the 1:2 compounds [M{N(SiMe$_3$)$_2$}$_2$]$_2$(4,4′-bipy) have not been successful to date. A similar experiment involving the reaction of Mn{N(SiMe$_3$)$_2$}$_2$ with the bidentate pyrazine ligand instead of 4,4′-bipy did not yield a 1:1 adduct. Instead the 2:1 species **1b**, which is very similar in structure to **1a**, was isolated.

3.2. Structures and spectra

The structures of seven of the eight complexes **1**–**5** (except **2b**) were determined by X-ray crystallography. Selected bond lengths and angles for **1**–**5** together with data for [Mn{N(SiMe$_3$)$_2$}$_2$(4,4′-bipy)·THF]$_\infty$ (**6**) [10] are listed in Table 2. The structures of **1a**, **2a**, **3b**, **4**, and **5** are illustrated in Figs. 1–5. Inspection of the data for the bispyridine complexes **1a**, **2a**, **3a** and the bispyrazine complex **1b** show that they display very large deviations from an idealized tetrahedral geometry as exemplified by the wide angles between the bulky amide ligands,

Table 2
Selected bond lengths (Å) and angles (°) for **1**–**5**

	1a	**1b**	**2a**	**3a**	**3b**	**4**	**5**	**6** [a]
Bond lengths								
M–N(1)	2.0588(8)	2.049(2)	1.9946(9)	1.984(1)	1.904(3)	1.979(2)	1.972(3)	2.048(3)
M–N(2)	2.0622(8)	2.035(2)	1.9959(9)	1.983(1)	1.904(3)	2.173(2)	2.111(3)	2.225(4)
M–N(3)	2.2531(9)	2.323(2)	2.180(1)	2.1135(1)	2.055(5)			
M–N(4)	2.2856(9)	2.314(2)	2.205(1)	2.115(1)				
N(1)–Si(1)	1.7113(9)	1.707(2)	1.7171(9)	1.712(1)	1.701(3)	1.719(2)	1.715(3)	1.709(3)
N(1)–Si(2)	1.7073(9)	1.715(2)	1.7195(9)	1.718(1)	1.711(3)	1.715(2)	1.716(3)	1.707(3)
N(2)–Si(3)	1.7101(8)	1.715(2)	1.7165(9)	1.717(1)				
N(2)–Si(4)	1.7097(9)	1.709(2)	1.7190(9)	1.712(1)				
Bond angles								
N(1)–M(1)–N(2)	127.18(3)	130.82(7)	127.07(4)	123.17(4)	140.7(2)			
N(3)–M(1)–N(4)	86.77(3)	96.23(7)	86.34(4)	90.1(4)	109.7(1), 109.7(1)			
Si(1)–N(1)–Si(2)	123.37(5)	122.63(10)	122.68(5)	122.06(6)	126.2(2)	122.10(9)	121.3(2)	123.1(2)
Si(3)–N(2)–Si(4)	123.50(5)	124.67(10)	122.59(5)	122.04(6)				
N(1)–M–N(1)′						126.44(9)	122.4(2)	128.0(1)
N(2)–M–N(2)′						87.62(8)	91.2(2)	

[a] Data from Ref. [10].

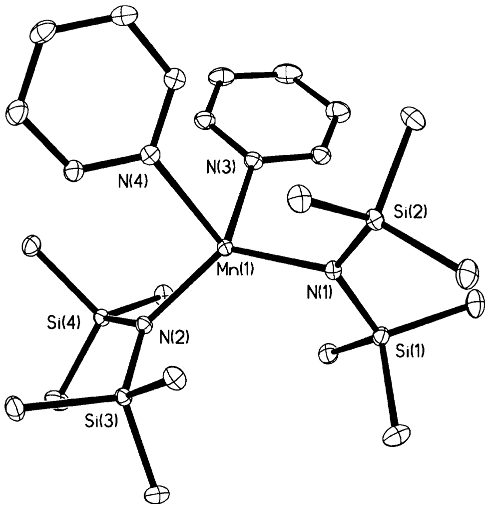

Fig. 1. Thermal ellipsoid plot (30%) of Mn$\{N(SiMe_3)_2\}_2(py)_2$, **1a**. H atoms are not shown.

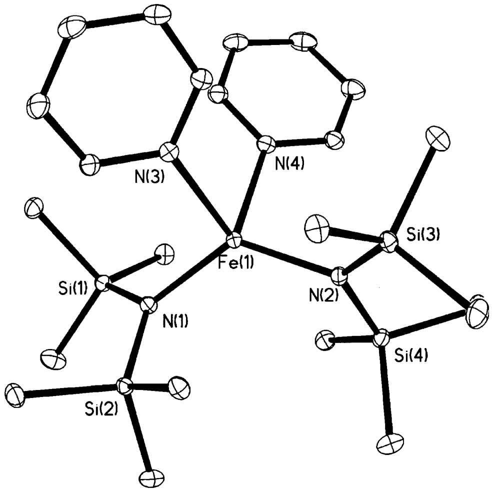

Fig. 2. Thermal ellipsoid plot (30%) of Fe$\{N(SiMe_3)_2\}_2(py)_2$, **2a**. H atoms are not shown.

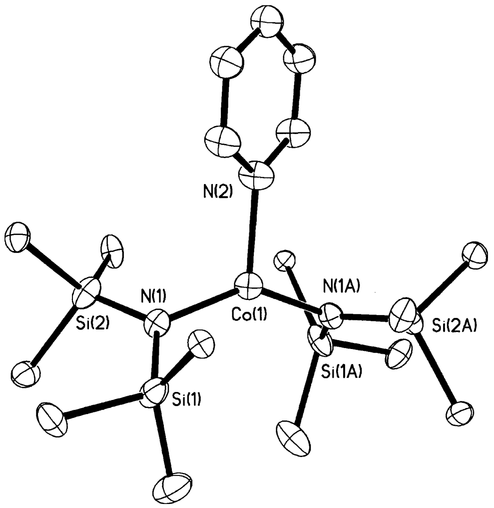

Fig. 3. Thermal ellipsoid plot (30%) of Co$\{N(SiMe_3)\}_2$py, **3b**. H atoms are not shown.

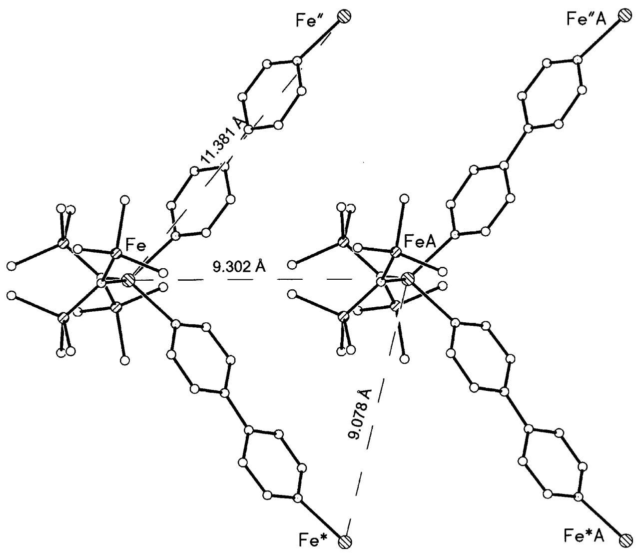

Fig. 4. Drawing of a section of the polymeric chain structure of **4** illustrating the closest intermetallic approaches.

123.17(4)°–130.82(7)° and the narrow angles 86.77(3)°–96.23(7)° between the pyridine or pyrazine ligands. The Mn–N(amide) bond lengths in the bispyridine and bispyrazine complexes **1a** and **1b** are similar, but slightly longer distances (by ca. 0.015 Å) were observed for **1a**. On the other hand the M–N(py) distances in **1a** (ca. 0.05Å) are shorter than those to the pyrazine ligand in **1b**. These differences may be interpreted in terms of weaker donor characteristics of pyrazine in comparison to pyridine. The Mn–N (amide) bond lengths and interamide ligand bond angles in **1a** and **1b** are very similar to those observed in Mn$\{N(SiMe_3)_2\}_2(THF)_2$ (Mn–N = av. 2.041(8) Å and N–Mn–N = 131.7(2)°) [9]. The structural parameters of the manganese, iron and cobalt bispyridine complexes **1a**, **2a** and **3a** display shorter M–N bonds in the sequence **1a** > **2a** > **3a** and this is in agreement with the relative sizes of the cations—$Mn^{2+} > Fe^{2+} > Co^{2+}$ [19]. The M–N (amide) bond lengths in **3a** compounds may be compared with those found in the corresponding monopyridine complex **3b** and in the previously reported compound and Co$\{N(SiMe_3)_2\}_2(PPh_3)$ (Co–N = av. 1.928 Å) [8]. Essentially, the M–N bonds in the three coordinate complexes are shorter than those in the four coordinate complexes by a margin of 0.06–0.09 Å. These differences are very similar to those observed for the pairs Mn$\{N(SiMe_3)_2\}_2(THF)_2$ [9] and Mn$\{N(SiMe_3)_2\}_2(THF)$ [11] and can be attributed to the decreased steric crowding and increased attraction between the transition metal ion and ligands in the three coordinate species. The Co–$N(SiMe_3)_2$ distance in three coordinate **3b**, 1.904(3) Å is approximately 0.024 Å

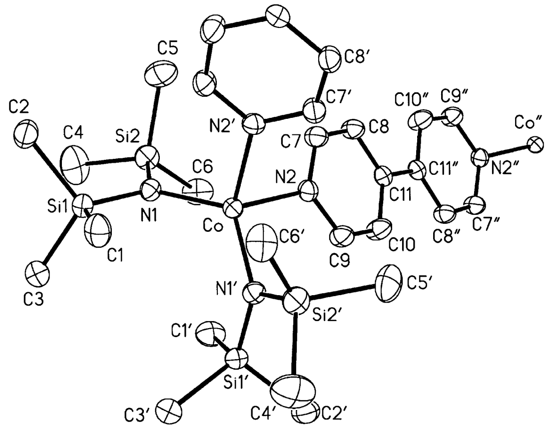

Fig. 5. Thermal ellipsoid plot (30%) illustrating to cobalt environment in **5**.

shorter than the 1.928 Å in Co{N(SiMe$_3$)$_2$}$_2$(PPh$_3$) [8], perhaps for steric reasons.

The X-ray structure of the isomorphous crystals of the 4,4′-bipyridyl complexes **4** and **5** possess zig-zag chains of M{N(SiMe$_3$)$_2$}$_2$(4,4′-bipy) units in which the metals are connected by opposite ends of the 4,4′-bipyridyl ligands (Figs. 4 and 5). The polymeric chain structure is propagated through an inversion center in the middle of the C(11)–C(11)′ bond which connects the rings of the 4,4′-bipyridyl ligand. A twofold axis of symmetry is also present, as crystallographically required, so that only one –N(SiMe$_3$)$_2$, a NC$_5$H$_4$ moiety (half the 4,4′-bipyridyl ligand) and the metal are required to define the structure. The iron and cobalt centers are separated by 10.122 and 11.275 Å within the chains. However, there exist closer approaches between the iron (9.078 and 9.302 Å, Fig. 4) and the cobalt (9.111 and 9.268 Å) centers of adjacent chains in each compound. It is notable that the in-chain separations given above are close to the 11.577 Å reported for the manganese analogue [Mn{N(SiMe$_3$)$_2$}$_2$(4,4′-bipy)·THF]$_\infty$, **6**, [10] although interchain Mn–Mn distances were not cited. The N(2)–C(11)–C(11′)–N(2′) array defines a straight line, but there are angles of 14.5° (Fe) and 11.7° (Co) between the M–N(2) bond and the extended C(11)–N(2′) vector. The aromatic rings of the 4,4′-bipyridyl ligand are coplanar as required by symmetry. The Fe–N and Co–N distances are marginally shorter (by just over 0.01 Å or ca. seven standard deviations) than these observed in **2a** and **3a**. On the other hand, the distances to the 4,4′-bipyridyl ligand nitrogen are approximately 0.06 Å longer than the distances to the pyridines in the complexes **2a** and **3a**. The interamide ligand N–M–N angles in the iron complexes **2a** and **4** and cobalt complexes **3a** and **5** differ by less than 1° while the corresponding angles between the pyridine or 4,4′-bipyridyl donors differ by 1.3 and 1.1°, respectively. In effect, the structural parameters surrounding the metal atoms in **4** and **5** resemble those of **2a** and **3a** very closely. It is apparent that the 4,4′-bipyridyl ligands achieve sufficient spacing between the hindered metal centers such that no increase in crowding over that present in **2a** and **3a** is observed. This is in obvious contrast to the case of **1b** where the use of the bidentate pyrazine ligand and the largest of the three metal ions Mn^{2+} do not permit polymerization to occur owing to the much greater steric crowding that would ensue due to the much shorter distance between the donor nitrogens.

3.3. Magnetic studies

Magnetic studies of crystalline samples of **1a**, **2a**, **3b**, **4** and **5** were undertaken in order to compare their behavior. The magnetization data were fit to a modified Curie–Weiss Law $\chi = \chi_0 + C/(\tau - \theta)$ where C is the Curie constant, θ is the Curie temperature. The effective moment was calculated from the relationship $\mu_{\text{eff}} = (8C)^{1/2}$. The μ_{B} values for **1a**, **2a** and **3b** indicate that they are all high spin with five, four and three unpaired electrons, respectively. The values for complexes **2a** and **3a** are near the upper limit of values observed for Fe^{2+} and Co^{2+} and indicate considerable orbital contributions to the magnetic moment. In contrast the μ_{B} values for **4** and **5** are significantly lower and slightly lower than the predicted spin only values which might suggest coupling between the paramagnetic centers. However, as is apparent from Fig. 6, the plot of $1/\chi$ versus temperature reveals a strictly linear relationship in the range 5–300 K. This indicates the magnetic coupling is close to zero and that the 4,4′-bipyridyl ligand does not apparently facilitate exchange between the paramagnetic atoms.

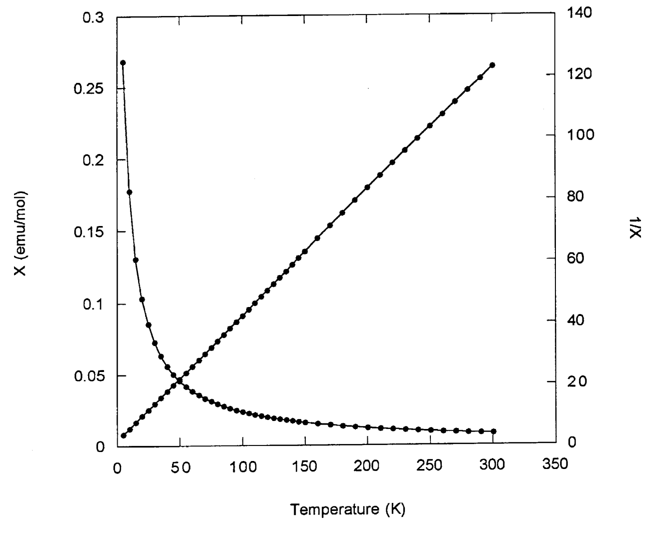

Fig. 6. Plots of χ (left hand ordinate) and $1/\chi$ vs. temperature for **4**.

4. Supplementary material

Crystallographic data for the structural analyses have been deposited with the Cambridge Crystallographic Data Centre CCDC Nos. 189463–69 for compounds **1**–**6**. Copies of this information may be obtained from The Director, CCDC, 12 Union Road, Cambridge, CB2 1EZ, UK (fax: +44-1233-336033; e-mail: deposit@ccdc.cam.ac.uk or www http://www.ccdc.cam.ac.uk).

Acknowledgements

We are grateful to the Donors of the Petroleum Research Fund administered by the American Chemical Society and UC MEXUS-CONACYT for financial support.

References

[1] H. Bürger, U. Wannagat, Monatsh. Chem. 94 (1963) 1007.
[2] (a) H. Bürger, U. Wannagat, Monatsh. Chem. 95 (1964) 1098; (b) D.C. Bradley, K.J. Fisher, J. Am. Chem. Soc. 93 (1971) 2058.
[3] R.A. Andersen, K. Faegri, J.C. Green, A. Haaland, M.F. Lappert, W.-P. Leung, K. Rypdal, Inorg. Chem. 27 (1988) 1782.
[4] P.P. Power, Chemtracts-Inorg. Chem. 6 (1994) 181.
[5] D.C. Bradley, M.B. Hursthouse, K.M. Abdul Malik, R. Möseler, Transition Met. Chem. (London) 3 (1978) 353.
[6] B.D. Murray, P.P. Power, Inorg. Chem. 23 (1984) 4584.
[7] M.M. Olmstead, P.P. Power, S.C. Shoner, Inorg. Chem. 30 (1991) 2547.
[8] D.C. Bradley, M.B. Hursthouse, R.J. Smallwood, A.J. Welch, Chem. Commun. (1972) 872.
[9] D.C. Bradley, M.B. Hursthouse, A.A. Ibrahim, K.M. Abdul Malik, M. Motevalli, R. Möseler, H. Powell, J.A. Runnacles, A.C. Sullivan, Polyhedron 9 (1990) 2959.
[10] M. Andruh, H.W. Roesky, M. Noltemeyer, H.-G. Schmidt, Z. Naturforsch., Teil. B 47 (1994) 31.
[11] P.G. Eller, D.C. Bradley, M.B. Hursthouse, D.W. Meek, Coord. Chem. Rev. 24 (1977) 1.
[12] B. Horvath, R. Möseler, E.G. Horvath, Z. Anorg. Allg. Chem. 450 (1979) 165.
[13] Quantum Design, Inc., San Diego, CA, 92121.
[14] H. Hope, Prog. Inorg. Chem. 41 (1995) 1.
[15] SHELXTL PC version 5.1; Siemens Analytical X-ray Instruments Inc., Madison, WI, 1994.
[16a] G. Sheldrick, SADABS (Siemens Area Detection Absorption Correction Program), Madison, WI, 1996.
[16b] S. Parkin, B. Moezzi, H. Hope, J. Appl. Crystallogr. 28 (1995) 53, XABS2.
[17] J.L. Sebestl, T.T. Nadasi, M.J. Heeg, C.H. Winter, Inorg. Chem. 37 (1998) 1289.
[18] K.J. Fisher, Inorg. Nucl. Chem. Lett. 9 (1973) 921.
[19] R.D. Shannon, Acta Crystallogr. 32 (1976) 751.